

## Evaluation of Mobile GSM Performance under Different Atmospheric Propagation Models

Qaysar S.Mahdi<sup>1</sup> & Idris H.Salih<sup>2</sup>

<sup>1</sup> Ishik University, IT Services Department, Erbil, Iraq

<sup>2</sup> Ishik University, Rectorate, Erbil, Iraq

Correspondence: Qaysar S. Mahdi, Ishik University, Erbil, Iraq.

Email: qaysar.mahdy@su.edu.krd

Received: October 12, 2017 Accepted: November 24, 2017 Online Published: December 1, 2017

doi: 10.23918/eajse.v3i2p151

**Abstract:** Atmospheric propagation is very effective on the performance of the wireless, mobile, radar, and communication systems. In this paper different atmospheric models are constructed under different atmospheric conditions. The performance of a GSM mobile communication is tested under different atmospheric models. From the obtained results, it is noticed that the coverage of the mobile system antenna is changed highly if the refractive index model of certain country is changed. It is concluded that the atmospheric propagation is very essential parameter to be taken into account when the siting of a mobile GSM network is to be evaluated and designed. This study will be very useful in order to predict the performance of ground radio and airborne systems.

**Keywords:** Atmospheric Models; Ducting Types; GSM Mobile; Performance

### 1. Introduction

There are several kinds of radio waves, such as ground, space, sky, and tropospheric waves, as shown in Figure 1. As the name indicates, the ground wave propagates along the surface of the earth, and the sky wave propagates in the space but can return to earth by reflection either in the troposphere or in the ionosphere. Different wavelengths are reflected to dissimilar extent in the troposphere and ionosphere. Based on the attributes of these waves, we can partition the spectrum which is based on propagation properties and the system aspects.

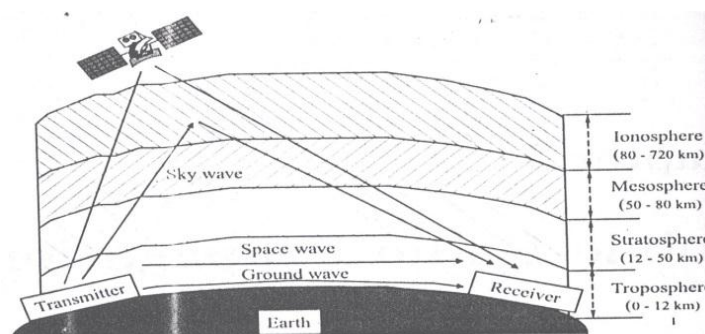


Figure 1: Propagation of different types of radio waves (Aziz, 2008)

## 2. GSM Mobile Radio Wave Propagation

The radio propagation of GSM mobile network is shown in Figure 2.

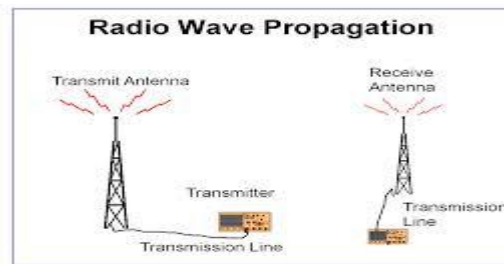


Figure 2: GSM mobile radio wave propagation network

Radio waves near the earth's surface do not usually propagate in precisely straight lines, but follow slightly curved paths. The reason is well-known to VHF/UHF users: refraction in the earth's atmosphere (Aziz, 2008; Pei, 2001; Barry). Refraction is the bending of the radio waves due to changes in the characteristics of the atmosphere. The atmosphere changes in temperature, density, and humidity as the altitude from the earth's surface increases. The change in density, in a way, also affects the velocity of microwaves traveling through the atmosphere (Barry). The formula for calculating the velocity is as in equation (1) where  $n$  the refractive index is (Aziz, 2008).

$$\text{Velocity (v)} = \frac{c}{n} = \frac{c}{\sqrt{\epsilon_r}} \quad (1)$$

## 3. Atmospheric Refraction

The propagation of electromagnetic waves has been actively studied for over 75 years with a number of objectives. These include telecommunication and television coverage prediction, microwave link design, studies of GSM mobile radio communication, and radar performance and design studies. The performance of mobile communication depend not only on the system design parameters but also on a number of other factors which have to be accounted for when assessing or predicting it.

## 4. Classification of Atmospheric Refraction

The bending in these circumstances is downward toward the earth, which allows the microwaves to be transmitted further than the direct straight-line path by tilting the antennas slightly upward. This is equivalent to increasing the radius of the earth's curvature (Pei, 2001). In practice, this allows a propagation path length that is approximately 15 percent longer than L.O.S path as shown in Figure 3 (Aziz, 2008; Pei, 2001). Refractive conditions are categorized into four basic classifications: Normal (standard atmosphere), and anomalous propagation (AP) Super-refractive, Trapping (Ducting), and Sub-refractive.

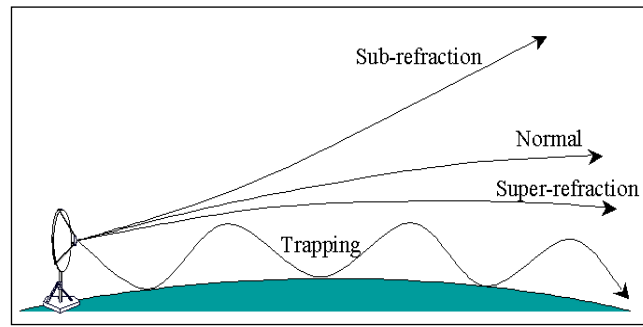


Figure 3: Four classification of refraction (Aziz, 2008)

However, due to the inherent variability of the atmosphere, it is a well-known fact that propagation conditions may differ, sometimes significantly, from those considered standard resulting in anomalous propagation (AP). As illustrated schematically in Figure 4, sub-refraction causes the radar beam to bend less than usual, and therefore follows a higher trajectory than in normal conditions. Super refraction of a ray beam produces more bending towards the ground surface than expected for standard conditions and therefore increases and intensifies ground clutter echoes (AP or anomalous propagation). An extreme case of super-refraction, known as ducting, occurs when the beam has a curvature smaller than that of the Earth surface (Bech et al., 2012).

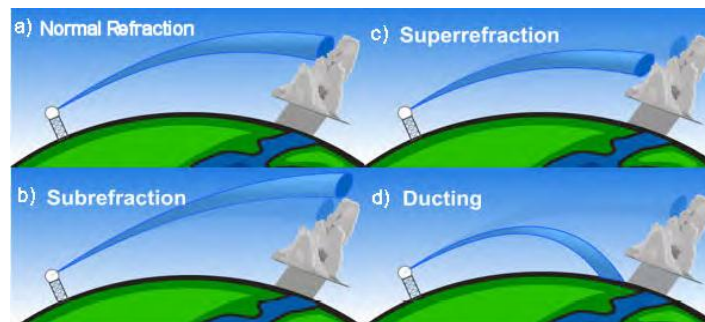


Figure 4: Radio beam propagation conditions (Bech et al., 2012)

#### 4.1 Definition of Ducting

Ducting is the abnormal propagation of electromagnetic waves. A decrease in the atmospheric index of refraction with increasing altitude bends the mobile or radar rays so as to extend the coverage beyond that expected with a uniform atmosphere. A refractive index gradient =  $- 1.57 \times 10^{-7} \text{ m}^{-1}$  will make the effective earth's radius infinite which allows initially horizontal rays to follow the curvature of the earth. Under such conditions, the mobile range is significantly increased and detection beyond the horizon can result.

## 5. Types of Refraction

### 5.1 Standard and Non-Standard Refraction

Standard refraction occurs through the troposphere where the distribution of the water vapor and temperature is homogenous with height, thus gradual homogenous change of refractive index decreases with height by a gradient of  $-0.04 \times 10^{-6} \text{ m}^{-1}$  for the standard refraction. This gradient requires a correction factor of the value  $k = 4/3$  (AL-Samerai, 1988).

$$k = 1 / 1 + (r/n) \text{ dn/dh} \quad (2)$$

Non-standard refraction occurs when the refractive index change with height ( $\text{dn/dh}$ ) deviates from the standard refraction gradient, and for this case the correction factor  $k \neq 4/3$  (varies from 2 to  $\infty$ ). Ducting is called a non-standard propagation (AL-Samerai, 1988).

### 5.2 Ducting Phenomena

Ducting is defined as trapping of radio waves energy and guiding it like the guidance of radio waves by the waveguide and travel long distances far away from the radio horizon and suffering little fading in its. Ducting is also considered as the abnormal propagation of EM waves. Variations of meteorological conditions which cause variations in refractivity  $N$  include fluctuation in the temperature, water vapor pressure and atmospheric pressure. For example when the refractivity gradient  $\text{dN/dh}$  equals to  $-157 \text{ N units/km}$  ( $-48 \text{ N units/kft}$ ), the electromagnetic rays will bend to follow the curvature of the earth (see Figure 5). Therefore ducting conditions occurs when the refractivity gradient is less or equal to  $-157 \text{ N units/km}$  (AL-Samerai, 1988).

### 5.3 Ducting Condition

Ray propagating under a refractivity gradient equal to  $\text{dN/dz} = -157 \text{ N/km}$  is exactly parallel to the surface of the earth. Gradients of less than  $-157 \text{ N/km}$  produce ducting where the curvature of the rays exceeds the curvature of the earth and the wave travels for a very long distance behind the radio horizon (Valtr & Pechac, 1987, 2005).

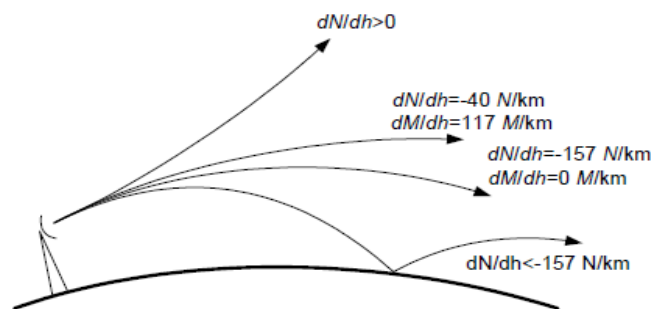
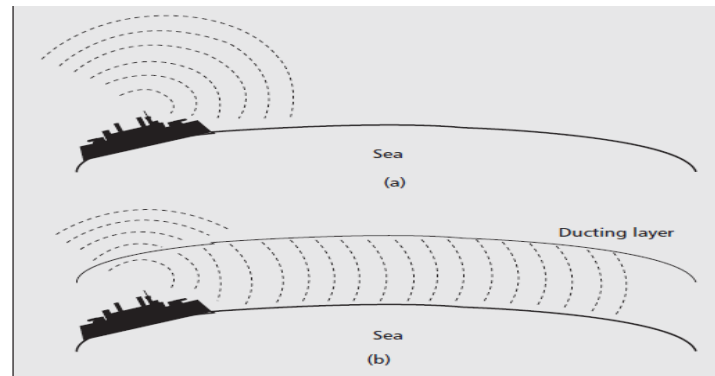


Figure 5: Rays under various refractivity gradients (Valtr & Pechac, 2005)

As a result, the spreading loss decreases considerably compared to the standard atmosphere, and there is a significant amount of increase in the received signal power. In this way, the trapped signals can travel over the horizon, making the ducting layer convenient for beyond-line-of-sight (b-LoS)

communications as shown in Figure 6.



**Figure 6:** Signal spreading in

a) the standard atmosphere; b) the atmospheric duct (Dinc & Akan, 2014)

As a result, the ducting layer communication becomes the dominant propagation mechanism at the lower troposphere, especially between 2 and 20 GHz. Since the transmitter and receiver antennas should be located within the ducting layer and this mechanism is effective at the lower troposphere, naval communications can especially utilize b-LoS communications with the ducting layer (Ergin & Akan, 2014).

## 6. Modeling of Refractive Index

### a. Linear Model

A linear model of the refractive index can be expressed as (AL-Samerai, 1988).

$$N(h) = a_1 + b_1 h \quad (3)$$

Where  $N(h)$  = The refractivity in N units as a function of height.

$a_1 = N_s$ , the surface value of N.

$b_1 = dN/dh$ , the refractivity gradient N units per km.

$h$  = The altitude above sea surface.

This model was constructed using a set of data refractometer measurements, and it may represent the refractivity at certain atmosphere condition. The surface refractivity ranges are from 240 to 400 N units and the average value of  $b_1$  is -35 N units/km (AL-Samerai, 1988).

### b. Modified Refractive Earth's Radius Model

The effective – earth's radius model, although very useful for engineering practice, is not very good representation of actual atmosphere N structure (AL-Samerai, 1988).

### c. Exponential Model

This model of the atmosphere may be specified by assuming a single exponential distribution of N (AL-Samerai, 1988):

$$N(h) = a \text{ Exp}(-bh) \quad (4)$$

Where,  $a$  = the surface refractivity  $N_s$  in N units,  
 $b$  = Constant per km

**d. Effects of Refractive Index on Mobile GSM Radio Propagation**

The correction factor  $k$  is given by (AL-Samerai, 1988):

$$k = 1 / 1 + (r/n) \text{ dn/dh} \quad (5)$$

where  $n$  = The refractive index which is assumed to be 1.000000.

$r$  = The earth's radius which is equal to 6371.220 km.

$\text{dn/dh}$  = The gradient of refractive index per km.

The  $k$  factor is linear for constant refractive index gradient) (i.e.,  $\text{dn/dh}$  constant), and a function of height for the case of the exponential model i.e.,  $\text{dn/dh} \neq$  constant but function of height).

**e. Linear Model**

The variation of the modified refractivity with height for the linear model can be obtained from Eqn. (15);

$$M(h) = n_1 + b_1 h + (h/r) 10^6 \quad (6)$$

**Case 1:**

$a_1$  – Positive constant = 300 N units.

$b_1$  – Assumes negative values

At height  $h = 0$ ,  $M(0)$ ,  $a_1 = N_s$ . Then  $M(h)$  changes linearly with height for all the assumed values of  $b_1$  see Figure. 7.

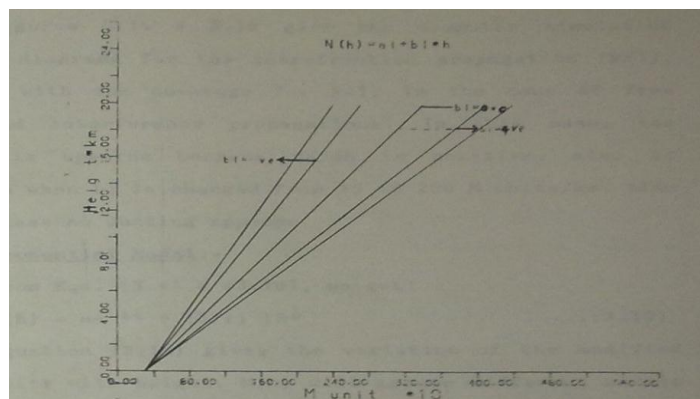


Figure 7: Modified Refractivity & height profiles

**Case 2:**

$a_1$  = Positive constant = 400 N units/km.

$b_1$  = Assumes positive values.

In this case the bending is upwards because  $\text{dN/dh}$  is positive; also it increases when  $b_1$  is changing from 35 to 200 N units/km. Also in this case no ducting appears.

**f. Exponential Model**

The modified refractivity for the exponential model is given by;

$$M(h) = a e^{-bh} + (h/r) 10^6 \tag{7}$$

Equation (16) gives the variation of the modified refractivity with height.  $M(h)$  will assume different models as shown in Figure. 8, depending on the values and sign of  $a$  and  $b$  in Eqn. (16).

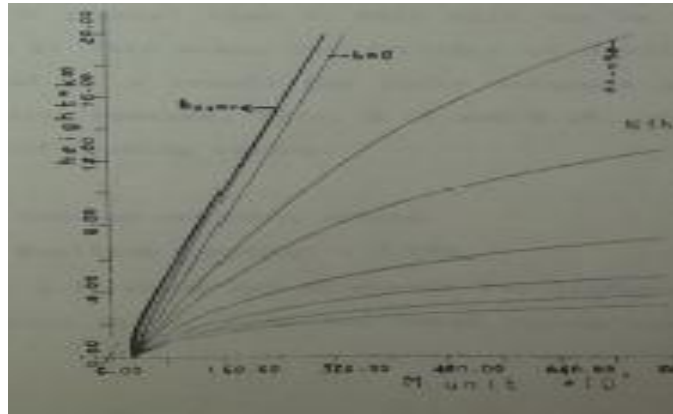


**Figure 8:** Modified refractivity & height profiles.

**Case 1:**

- a = Positive constant = 300 N units.
- b = Positive values.

For  $h = 0$ ,  $M(0) = a = Ns$ . The gradient of  $M(h)$  will be negative for a certain ranges of  $h$  depending on the value of  $b$ , then for higher values of  $h$  the slope will change to positive, see Figure. 8. The minimum value of  $M(h)$  will depend on the assumed value of  $b$ .

**Case 2:**

- a = Positive constant = 300 N units.
- b = Assumes negative values

For  $h$  greater than 0,  $M(h)$  will not be less than  $a$  i.e.  $M(h) > a$ .

**Case 3:**

- a = Assumes positive values.
- b = Positive constant = 0.999

Figure 9 shows set of curves for different values of  $a$  and constant value of  $b$ , and these curves are plotted in a logarithmic scale, in order to clarify the law altitudes.

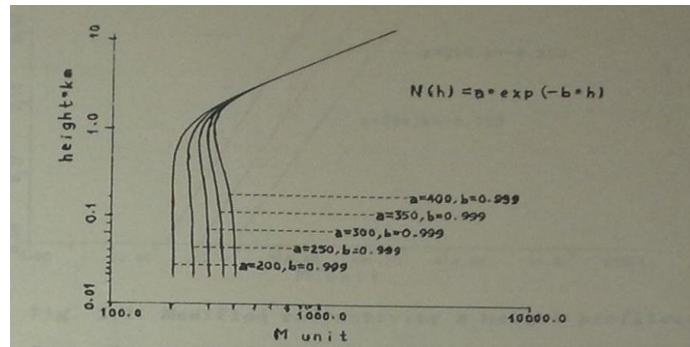


Figure 9: Modified refractivity & height profiles

**Case 4:**

- a = Assume positive values.
- b = Assumes negative constant = -0.353 per km.

The modified refractivity profiles for different values of a are shown in Figure 10.

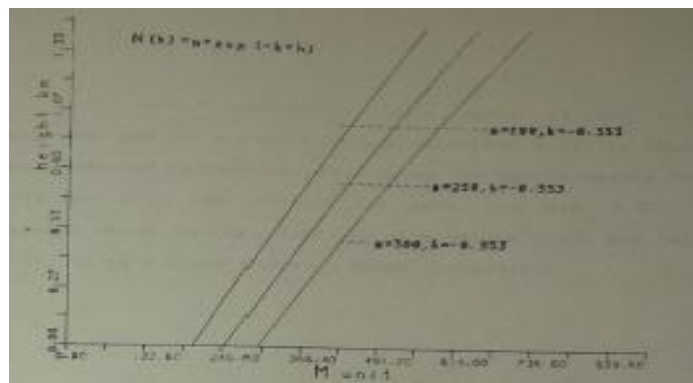


Figure 10: Modified refractivity & height profiles.

From Eqn. (16), the gradient of the modified refractivity for this case can be expressed as:

$$dM/dh = - a b e^{-b h} + 10^6/r \tag{8}$$

**g. Modeling & Ray Tracing**

All ray tracing methods in refractive media are based either on Snell`s law or Fermat`s principle. But Fermat`s also lead to Snell`s law. There are two methods for tracing the ray path, the stratified layer method and the integral method. In this study, ray paths are calculated by a ray tracing program which was developed to estimate the actual paths according to the refractivity profile. The approach based on a derivation of the Appleton differential equation of an EM ray propagating through a spherically stratified atmosphere with a describing refractivity relative to height, as follows (AL-Samerai, 1988):

$$\tan^2 \alpha_h = \tan^2 \alpha_o + 2 ( M_h - M_o ) 10^6 \tag{9}$$

Where M is given by Eqn. (20) and  $\alpha_h$  and  $\alpha_o$  are ray angles at heights h and  $h_o$  respectively. The process of ray tracing starts from the antenna where the first ray propagates with a lurching angle  $\alpha_o$ , a horizontal range equal to zero and a ray height equal to the antenna height  $h_o$ , Then the calculation

of the modified refractivity at this height is given by , ( The height  $h_1$  is modified by the radius of the earth  $r$  ):

$$M_1 = N_1 + (h_1 / r ) 10^6 \quad (10)$$

Where  $N_1$  the refractivity is at height  $h_1$ . The new ray height at a new ground range is equal to the distance  $x_o$  away from antenna location;

$$h_2 = h_1 - x_o \tan \alpha_o \quad (11)$$

where  $\alpha_o$  is the apparent elevation angle.

At this stage a test is carried out to find whether the ray path makes a cross with the ground surface (i.e. reflection point), (assumed flat) or it is propagating normally through the troposphere. If the former case is true, the program consider the ray reflect from that point. But if no reflection occurs, i.e. the latter case, the program proceeds in evaluating the modified refractivity at the new ray height  $h_2$  .

$$M_2 = N_2 + (h_2 / r ) 10^6 \quad (12)$$

Where  $N_2$  is the refractivity at level  $h_2$  . Then the ray angle can be evaluated by employing Eqn. (20) as;

$$\alpha_h = \tan^{-1} ( \tan^2 \alpha_o + 2 \Delta M ) 10^{-6} )^{1/2} \quad (13)$$

#### **h. The Maximum Launching Angle for Ducting**

The ray trajectory again change concavity where the M-profile slope changes and is again horizontal at height A, being refracted upward at this height.

The critical trapping angle is given by:

$$\alpha_c = \pm \sqrt{2 | \Delta M | } \text{ mrad} \quad (14)$$

The maximum launching angle for ducting can be function of the refractivity gradient and the duct depth as given by:

$$\alpha_c = \pm (2D)^{1/2} ( -0.157 - dN/dh )^{1/2} 10^{-3} \quad (15)$$

where  $D$  = The duct depth in meters,

$dN/dh$  = The refractivity gradient in N units per meter.  $\alpha_c$  is plotted as function of duct depth and refractivity gradient in Figure.11.

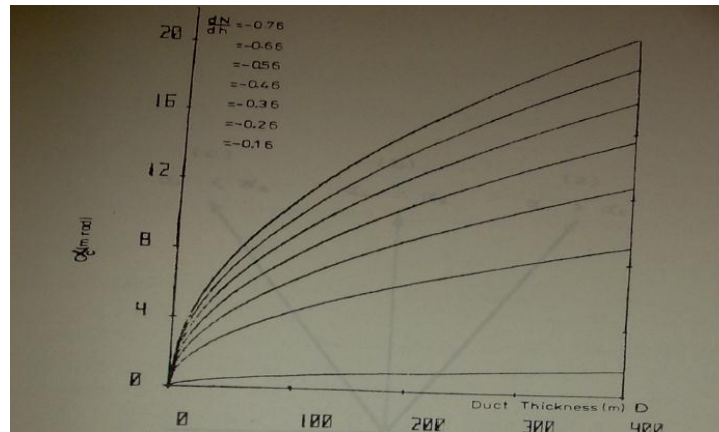


Figure 11: Critical launching angle and the duct depth

Figure 12 gives the limits of critical launching angle for ducting. Assuming a ground-based duct, let us consider  $M_0$  be the modified refractivity at the source point, if  $M$  is positive,  $\alpha_h > \alpha_c$  as in case (a) of Figure.12, and in this case the ray does not bend towards the ground. And if  $M=0$ ,  $\alpha_h = \alpha_c$ , as in case (b) of Fig.12, so the ray keeps constant launching angle, but if  $M$  is negative,  $\alpha_h < \alpha_c$  as in case (c) of Figure.12, the ray bends towards the ground.

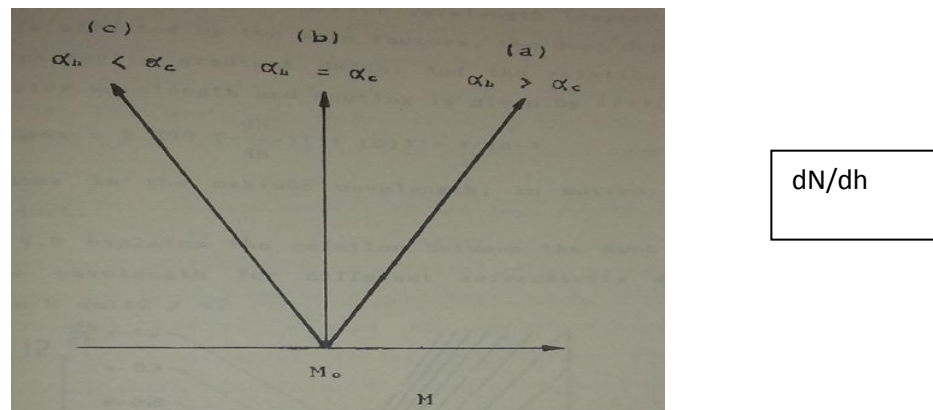


Figure 12: The limits of the critical launching angle for ducting (AL-Samerai, 1988)

The practical value of  $\alpha_c$  is from -0.5 degree, and the maximum and minimum values of  $\alpha_c$  for Baghdad city along 10 years measurements are found to be 8.5 mrad ( 0.49°) and 0.35 mrad ( 0.02°) respectively.

### i. Relation between Carrier Wavelength and Ducting

The maximum mobile carrier wavelength trapped in into a duct is affected by two main factors, the duct depth  $D$  and the refractivity gradient  $dN/dh$ . And the relation between the carrier wavelength and ducting is given by,

$$\lambda_{\max} = 2.296 ( dN/dh )^{1/2} ( D )^{3/2} * 10^{-3} \quad (16)$$

Where  $\lambda_{\max}$  is the maximum wavelength, in meters, trapped into a duct. Figure 13 explains the

relation between the duct depth  $D$  and the wavelength for different refractivity gradient,  $dN/dh$  in N units/m.

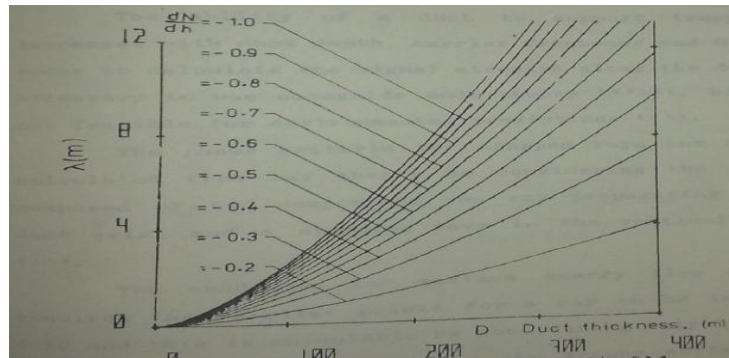


Figure 13:  $\lambda_{\max}$  and duct depth

From Figure 13, the bending of radio waves will be high if the gradient  $dN/dh$  is high (in the negative), also as high as duct depth, the ray path will be longer through the duct depth, so the ray also bends towards the ground. Also at certain level the value of  $\lambda_{\max}$  changes greatly with the change of the modified refractivity, therefore it is possible to know the range of the mobile wavelengths which are affected by duct depth. The practical values of  $\alpha_c$  and  $\lambda_{\max}$  for Baghdad city are shown in Table 1. These values are considered for different duct conditions over a period of 10 years (ALSamerai, 1988).

Table 1: Measurements of duct condition for Baghdad City along 10 years

| Date | $dN/dh$<br>(Nunits/m) | D<br>(m) | $\alpha_c$<br>(deg.) | $\lambda_{\max}$<br>(m) |
|------|-----------------------|----------|----------------------|-------------------------|
| 16-3 | -0.19                 | 089      | 0.14                 | 0.38                    |
| 23-3 | -0.196                | 136      | 0.19                 | 0.78                    |
| 5-4  | -0.171                | 148      | 0.12                 | 0.53                    |
| 16-4 | -0.21                 | 089      | 0.18                 | 0.48                    |
| 17-4 | -0.159                | 232      | 0.5                  | 0.39                    |
| 18-4 | -0.201                | 159      | 0.21                 | 1.1                     |
| 20-4 | -0.175                | 116      | 0.12                 | 0.42                    |
| 23-4 | -0.206                | 137      | 0.21                 | 0.89                    |
| 8-5  | -0.187                | 74       | 0.12                 | 0.28                    |
| 12-5 | -0.316                | 85       | 0.3                  | 0.78                    |
| 27-5 | -0.185                | 122      | 0.15                 | 0.56                    |
| 5-6  | -0.19                 | 87       | 0.14                 | 0.37                    |
| 6-6  | -0.213                | 196      | 0.27                 | 1.62                    |
| 21-6 | -0.252                | 109      | 0.26                 | 0.88                    |
| 27-6 | -0.159                | 311      | 0.7                  | 0.61                    |
| 29-6 | -0.158                | 92       | 0.02                 | 0.05                    |
| 1-7  | -0.23                 | 98       | 0.22                 | 0.66                    |
| 2-7  | -0.226                | 235      | 0.33                 | 2.37                    |

#### j. Effects of Refractive Index Models on Ducting Phenomena

The modeling of the refractive index for the prediction of the propagation condition in certain country is on the vertical distribution of the temperature, relative humidity and pressure in that country. Each model has different profiles depending on the climatically and geographical parameters. The user is caution that as with many models, the real world may be uncooperative and deviate substantially. In this case, the model represents a long term global average of the atmosphere. Variations from this model occur seasonally, with changes of altitude, time of day, and rapid variations may also occur in local areas. The validity of each profile describing the duct condition for each country depends on the occurrence of constructing the constants of each model. As a result

good prediction of duct occurrence, will be produced, when higher accuracy of measurements is employed. The ducting phenomena is studied by using ray tracing technique, and examined for different refractive index models. These refractive index models are:

1. Linear model
2. Bilinear model
3. Trilinear model
4. Exponential model
5. S model

In this paper, a study of radio waves ducting is explained and examined for different atmospheric refractive index models. New ray tracing approach is used for the computation of the ray path. According to ray theory, five refractive index models affects the ducting phenomena are studied, such as linear, bilinear, trilinear, exponential and S models. These models are derived from observational data of different sites such as Baghdad, North Arabian Sea (NAS), Eastern Mediterranean Sea (EMS), Caribbean Sea and Central Pacific (AL-Samerai, 1988). For each model, the maximum wavelength and maximum launching angle for ducting condition were computed. Also effect of trapping layer on airborne mobile, having different tilts and altitudes, was examined for each model. Also in this paper, ray tracing approach was studied to predict the ducting and refraction of EM waves for linear and exponential refractive index models.

#### k. Effects of Ducting Layer on Airborne Mobile Radio System

Detection of airborne mobile radio system depends on many factors. One of the most factors is the propagation through a subrefractive or a ducting layer, see Figure.14. In this study the effect of the ducting layer on the airborne mobile radio will be studied.

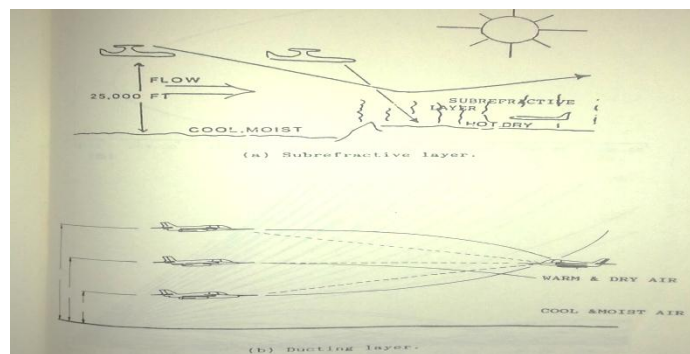


Figure 14: Airborne Mobile Radio Propagation under ducting layer condition (AL-Samerai, 1988)

Different models are used to examine the anomalous effects on airborne mobile radio. The mobile antenna assumed to have different tilts and altitudes. The mobile antenna half power vertical beamwidth is taken to be  $2^\circ$ . For each tilt, different altitudes are taken, in order to study the effect of the ducting layer on the propagation of mobile radio rays.

## 7. Results

Five models, linear, bilinear, trilinear, exponential and S, of refractive index were studied. Certain atmosphere conditions were simulated by exponential and linear models under the case of ground-based ducts. A comparison between exponential and bilinear, and also between S and trilinear refractive index models were presented in Table 2. The maximum trapping wavelength, maximum launching angle for trapping and minimum cut off frequency for trapping were calculated to explain the difference between models

**Table 1:** Calculation of Critical Launching angle for different Atmospheres

Antenna height = 60m, vertical beamwidth = 2°

| Model         | Atmosphere Area | $\alpha_c$ mrad |
|---------------|-----------------|-----------------|
| Bilinear      | Baghdad         | $\pm 6.3$       |
| Trilinear     | NAS             | $\pm 2.82$      |
| Trilinear     | EMS             | $\pm 18.33$     |
| Exponential   | Actual          | $\pm 8.29$      |
| Fitted – Expo | Actual          | $\pm 13.25$     |
| S             | Actual          | $\pm 3.99$      |
| Fitted - S    | Actual          | $\pm 19.95$     |
| IREPS         | Simulated       | $\pm 8.48$      |

- **Variation of GSM Mobile Antenna Height over Sea Level**

In order to evaluate the propagation of the GSM mobile radio in different atmospheric refraction index no =300 and ho=150m and the antenna heights height is changed for the following values.

**a. Antenna Height, ht= 75 m, no=300 and ho=150m**

In this case, some of the rays bend towards the earth surface for the heights lower than 100m which gives indication of the ducting propagation and the probability of detection will be increased. Also it is noticed that some of the rays are reflected upwards. For the heights above 180m, it is noticed that the rays bend upwards which gives indication of subrefraction and the probability of detection will be decreased. Figure 15, shows this case and it is seen that the reflected rays will interact the other rays which are bending upward.

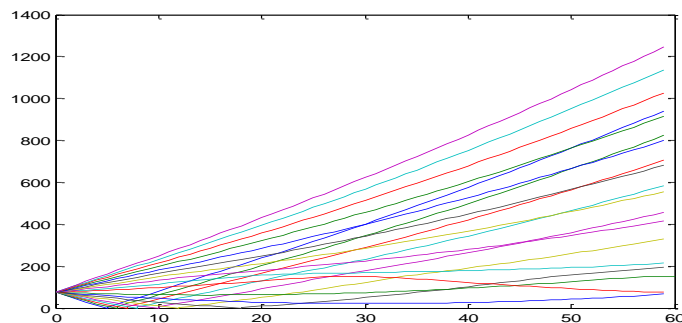


Figure 15: Antenna height , Ht= 75m

**b. Antenna Height  $h_t=1000$  m,  $n_o=300$  and  $h_o=150$  m**

In this case no ducting is appeared and the radio rays are all nearly straight lines and in the upper part nearly half the rays tend to bend upwards which indicate a subrefraction propagation and the lower part of the radio rays bend towards the ground which indicate normal propagation as shown in Figure 16.

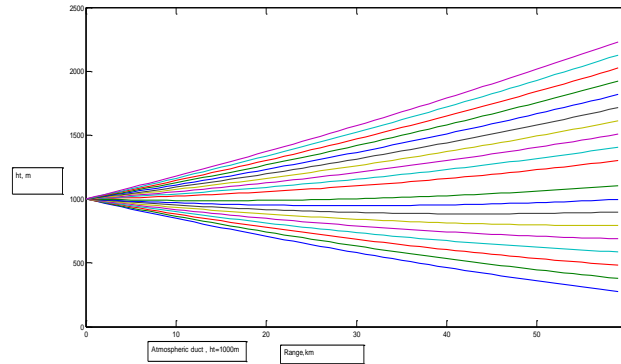


Figure 16: GSM antenna height  $h_t = 1000$  m

**c. Antenna Height  $H_t = 200$  m and  $dN/dh = 7.5$  N units/km**

In this case  $n_n=750$  for  $dh=100$  m which gives gradient of refraction equals to  $7.5$  N units /km. Also ducting propagation appears with first hope at reflection points  $19$  km, and the second ducting hope at range  $29$  km. Figure 17, shows that at height  $200$  m and below, the probability of detection increases.

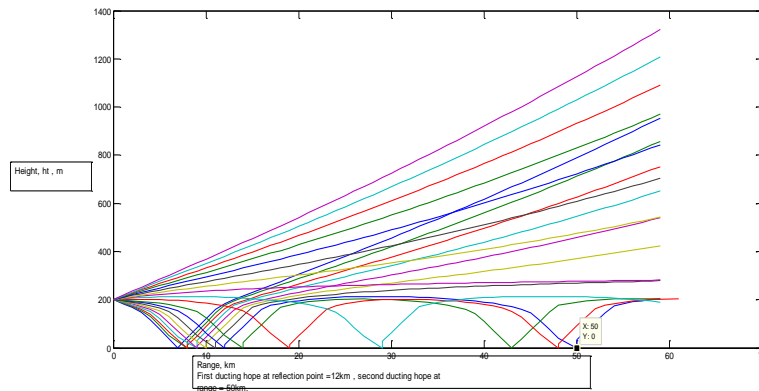


Figure 17: Antenna height,  $H_t = 200$  m,  $n_n=750$ ,  $dh=100$  m,  $h_o=150$  m,  $n_o=300$

**d. Antenna Height  $H_t = 200$  m and  $dN/dh = 9.375$  N units/km**

Here  $n_n=750$  and  $dh=80$  which gives  $dN/dh = 9.375$  N units/km. Figure 20, shows the number of ducting rays increases. The first ducting hope appears at range =  $22$  km, second ducting hope at range =  $40$  km, and third ducting hope at range =  $48$  km. Figure 18, shows this case.

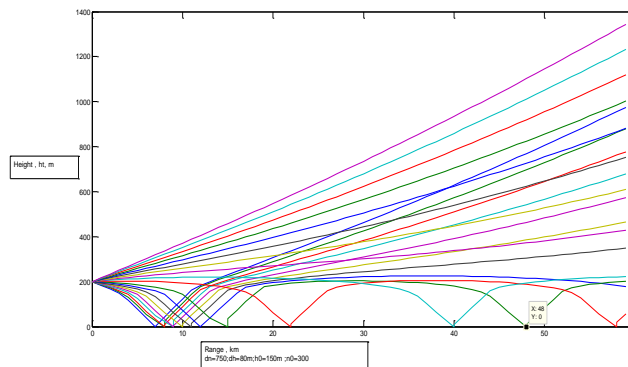


Figure 18: Antenna height  $H_t = 200\text{m}$ ,  $d_n = 750$ ,  $d_h = 80\text{m}$ ,  $h_o = 150\text{m}$ ,  $n_o = 300$

**e. Antenna Height  $H_t = 200\text{m}$  and  $dN/dh = -2.5 \text{ N units/km}$**

In this case  $d_n = -200$  for  $d_h = 80\text{m}$  and the refraction gradient  $dN/dh = -2.5 \text{ N units/km}$ . Here all the rays bend upwards and complete subrefraction propagation appears. Figure 19, shows no indication of ducting propagation.

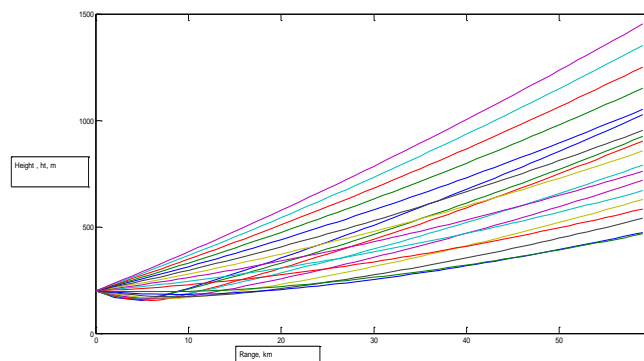


Figure 19: Antenna height  $H_t = 200\text{m}$ ,  $d_n = -200$ ,  $d_h = 80\text{m}$ ,  $h_o = 150\text{m}$ ,  $n_o = 300$

**f. Antenna Height  $H_t = 100\text{m}$  and  $dN/dh = 9.375 \text{ N units/km}$**

In this case the GSM height is changed from 200m to 100m and the refraction gradient is changed from positive value of  $-2.5 \text{ N units/km}$  to  $+1.25 \text{ N units/km}$ . A clear important change is noticed in Figure 20.

Most of rays are propagating in the ducting layer between 180m and earth surface and ducting propagation appears in this case instead of the subrefraction which is appeared in Figure 19. Some of the rays have subrefraction propagation. The probability of detection increases here highly and this will improve the GSM propagation performance.

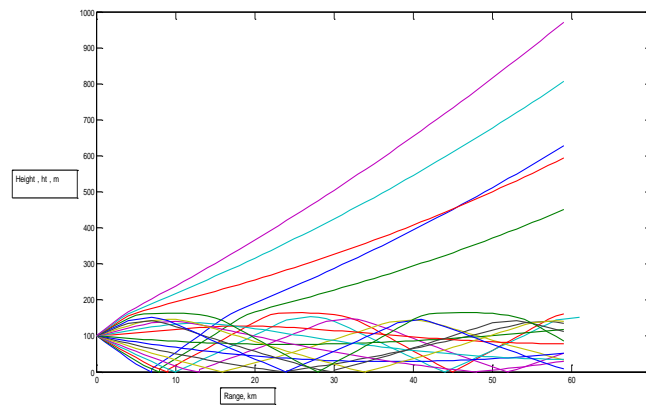


Figure 20: Antenna height  $H_t=100\text{m}$  ,  $d_n=100$ ;  $d_h=80$ ;  $h_0=150$ ;  $n_0=300$

## 8. Conclusion

In this study , different refractive index models are modeled and simulated such as ; linear, bilinear, trilinear, exponential and S models.

Ray tracing was employed to display the GSM mobile wave propagation under complex tropospheric environment. The vertical elevation beamwidth is  $2^\circ$ , was divided into 20 rays. These rays were traced, for certain rang, using different refraction gradients and heights. The critical launching angle, the maximum trapped wavelength and duct depth are calculated for different refractive index models.

One can conclude that GSM mobile receivers within the trapped layer the detection depend on the vector sum of the rays in the unit area. The vector sum gives maximum for inphase field components and minimum power density for out of phase components. Therefore, when the GSM receiver is moving along the duct it will be detected at one point and not detected at other. The criteria which gives inphase field components within the ducting layer depends on the duct depth, carrier wavelength, trapping mode number and modified refractivity profile. It was seen that if the trapping mode number  $m$  is 1 a maximum trapping carrier wavelength can be calculated, for certain duct depth the modified refractivity profile. Also the higher the duct depth, the lower the trapped carrier frequency. Therefore, one can conclude that the range of trapped frequencies depends on the duct depth, the modified refractivity profile and the trapping mode number. Like the waveguide, the range of frequencies propagating inside the waveguide depends on the depth of waveguide and the propagating mode of the EM field.

From the tests carried on the simulated airborne mobile radio it is clear that the receiver lose a tracked detection due to the maneuver of the airborne receiver, this is due to the trapping of rays in ducts or sudden bending of rays due to plane maneuver change of receiver altitude. In order to prevent the above disadvantages the airborne transceiver must carry the exact model of the refractive index of the complex environment panned for operation and include a special system to provide the correction with respect to the model.

This suggestion is not easily implemented because it requires fast, accurate and light equipment included to the airborne transceiver. And this suggestion could be an aim for future work.

## 9. Recommendation for Future Work

The subject of refraction of EM-waves in complex environment (topography and troposphere has many application in communication and radar systems. It has been found that there are little available published data about the refractive index models such as exponential and S models. This work can be extended to study:

1. The frequency range that affect the number of trapping rays within the ducting layer.
2. The prediction of the range within the duct at which detection is possible, and this leads us to study the vector sum of all rays propagating along the duct.
3. The number of possible trapped modes within the duct for polarization and refractivity profile.
4. The atmospheric attenuation on the EM waves propagating through the trapping layer. This affects the detection threshold within the duct.
5. Possibly of implementing a system to provide the error correction due to complex atmosphere variations and its effect on airborne mobile detection.
6. This work may be extended to study the ducting conditions in complex topography in order to introduce both the multipath and refraction effects (Mahdy & Aziz, 2010).
7. The exponential, bilinear, trilinear and S models effects on ducting conditions might be good work in order to predict the coverage of the mobile radio propagation.
8. Constructing the mobile and radar coverage by introducing the atmospheric and tropospheric models will give good prediction to their performance during ducting conditions.

## 10. Acknowledgement

We would like to express our gratitude thanks to Prof. Dr. Mahmood Alniamy, for his headlines and technical support. Also we express our thanks to the computer science center, MEC College, especially to Mr. Omar Al Azzawee and Mr. Haitham Polis for offering the facilities and programming . Also we would like to thank to the Meteorological Authority in Baghdad for providing us the required record of Baghdad atmosphere along 10 years.

## References

- AL-Samerai K.S. (1988). *Modeling of Radar Wave Propagation*. M.Sc. Thesis, MTC College.
- Aziz, A.M. (2008). *Software\_based\_DMC\_generation\_For\_UHF\_WirelessRadio\_propagation*. M.Sc., thesis, Dept. of Electrical Engineering, College of Engineering, Salahaddin University.
- Barry M. *VHF/UHF/Microwave Radio propagation: A primer for digital experimenters*. Retrieved from [http:// www.tapr.com](http://www.tapr.com).
- Bech, J., Magaldi, A., Codina, B., & Lorente, J. (2012). *Effects of Anomalous Propagation Conditions on Weather Radar Observation*. Dep. University of Barcelona, Institute of Space Sciences, Spanish National Research Council (CSIC), Bellaterra, Spain. Retrieved from <http://www.intechopen.com/download/35118>.
- Ergin, D., & Akan, O.B. (2014). *Beyond-Line-of-Sight Communications with Ducting Layer*. IEEE Communications Magazine.
- Mahdy, Q.S., & Aziz, A.M. (2010). *Software\_based\_DMC\_generation For UHF\_Wireless\_Radio\_propagation*. Antennas Propagation and EM Theory (ISAPE), 9th International Symposium (pp. 485 - 488), IEEE Conference Publications.
- Pei L.T. (2001). *Line-Of-Sight Ranging System*. Master Thesis, University of Queensland.
- Valtr, P., & Pechac, P. (2005). *Tropospheric Refraction Modeling Using Ray-Tracing and Parabolic Equation*. *Radio Engineering*, 14(4), 98-104.
- Valtr, P., & Pechac, P. (1987). The effects of various refractivity gradients. *Radio Engineering*, 35(1), 94-99.